

SOIL MODELS: SAFETY FACTORS AND SETTLEMENTS

Gabriella VARGA and Zoltán CZAP

Geotechnical Department
Budapest University of Technology and Economics
H-1521 Budapest, Hungary
e-mail: varga_gabriella@hotmail.com, zczap@mail.bme.hu

Received: Nov. 2, 2004

Abstract

Today's technology makes it possible to easily compute slope stability using computer software but the accuracy of the results is questionable. In this paper we compare how the application of three different models influences the results in case of different types of soil using the results of laboratory tests from several parts of Hungary. From the analysis of a cutting, soft-soil model deformations are much smaller than that of the other two models. The results of the calculation of an embankment are similar. The safety parameters are approximately the same for each model.

Keywords: soil model, laboratory test, clay, safety factor, settlement.

1. Introduction

Having heard of the presentation of Numerical analysis of deep excavations [2] drew our attention to the subject discussed in this paper. After thoroughly analysing the paper itself we found that their results do not match our findings, thus we decided to do further investigations [3]. This paper presents our results that are based on recent geotechnical soil models.

The fracture of soil is mainly caused by shearing and the formation of yield surfaces. Fractures can develop by loading and unloading. These two alternatives are shown in the following figures (*Fig. 1*).

In these states the elastic and plastic deformations can also be formed. It means that we have to use models that are valid for both the elastic and plastic zones. In order to be able to select the proper model we have used the results of several laboratory tests. Most of the examined soils were soft or hard clay.

We have done calculations using three different models: Mohr-Coulomb model, soft soil model, and the hardening soil model [1] (further details can be found in [4], [5], with the latter one discussing the PLAXIS program). In all three models we need to define the elastic and plastic yield conditions. The yield condition is the same for all the three models: that is the MC yield condition shown in the *Fig. 2*.

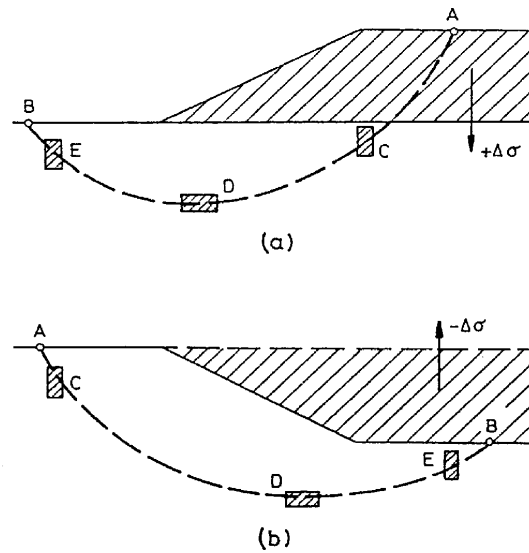


Fig. 1. Two alternatives of soil fracture a) loading b) unloading

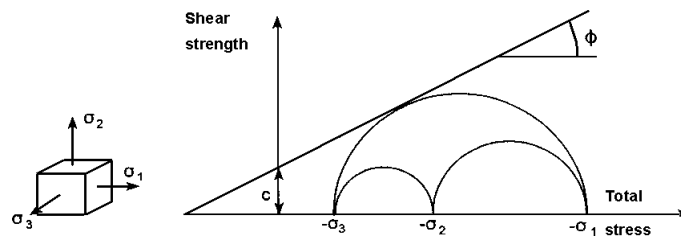


Fig. 2. Mohr-Coulomb Model

2. Mohr-Coulomb Model

The elastic-plastic Mohr-Coulomb model is a 'first order' approximation of soil behaviour. Since this model uses constant stiffness the calculation is quite fast. The model uses five parameters as well as the initial stress of the soil under examination:

- E , the Young's modulus (or E_{oed} , the oedometer modulus, or G , the shear modulus)
- ν , the Poisson's ratio,
- c , the cohesion,
- ϕ , the friction angle, and

- ψ , the dilatancy angle (only in dense cohesionless or overconsolidated cohesive soils).

Parameters are obtained from drained triaxial tests. In order to calculate the Young's modulus, E , the secant modulus at 50% strength denoted as E_{50} is recommended, the initial slope indicated as E_0 is only to be used if we make no use of the initial strength. (See Fig. 3).

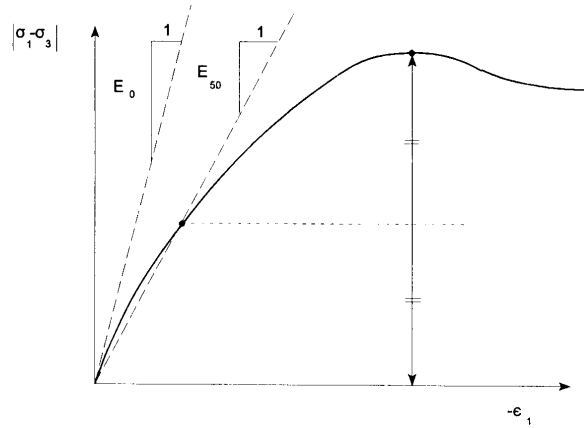


Fig. 3. The definition of the Young's modulus

3. Hardening-Soil Model

This model is fairly more accurate than the Mohr-Coulomb model for simulating the behaviour of different types of soil, both soft soils and stiff soils. In order to describe soil stiffness it makes use of the unloading and reloading stiffness as well as the oedometer loading stiffness. The hardening soil model is characterized by the stress-dependency of stiffness moduli. Based on the compression test the following formula can be used:

$$E_{\text{oed}} = E_{\text{oed}}^{\text{ref}} \left(\frac{\sigma}{p^{\text{ref}}} \right)^m,$$

where:

E_{oed} the oedometer modulus
 $E_{\text{oed}}^{\text{ref}}$ the reference oedometer modulus,
 p^{ref} the reference pressure.

The p^{ref} , reference pressure is typically 100 kPa. Another characteristic of this model, which is based on the triaxial test, is a hyperbolic dependency between

the vertical strain, ε_1 , and the deviator stress, q ($q = \sigma_1 - \sigma_3$).

$$-\varepsilon_1 = \frac{1}{2E_{50}} \frac{q}{1 - \frac{q}{q_a}}, \quad E_{50} = E_{50}^{\text{ref}} \left(\frac{c \cdot \text{ctg } \phi - \sigma_3'}{c \cdot \text{ctg } \phi + p^{\text{ref}}} \right)^m,$$

where

- q_a the asymptotic value of the shear strength,
- q the deviatoric stress,
- ε_1 the vertical strain,
- E_{50} the confining stress dependent stiffness modulus for primary loading,
- p^{ref} the reference pressure,
- E_{50}^{ref} the reference stiffness modulus corresponding to p^{ref} ,
- σ_3' the minor principal stress.

The ultimate deviator stress, q_f , and the asymptote, q_a are defined as:

$$q_f = (c \cdot \text{ctg } \phi - \sigma_3') \frac{2 \sin \phi}{1 - \sin \phi}, \quad q_a = \frac{q_f}{R_f},$$

where

R_f the failure ratio, is typically 0.9.

The unloading-reloading modulus (E_{ur}) varies as a function of σ_3' similarly to the E_{50} modulus. Typically $E_{\text{ur}}^{\text{ref}} = 3E_{50}^{\text{ref}}$. The dilatancy value is limited by the dilatancy cut-off.

4. Soft-Soil Model

The most important features of this model include stress-dependent stiffness, the differentiation between primary loading and unloading-reloading, the memory of pre-consolidation stress, and the usage of the Mohr-Coulomb criterion.

The equation for primary loading is:

$$\varepsilon - \varepsilon_{\text{ref}} = -\lambda^* \cdot \ln \left(\frac{p}{p_{\text{ref}}} \right),$$

where

λ^* the modified compression index.

The equation for unloading-reloading is:

$$\varepsilon_v^e - \varepsilon_v^{e0} = -\kappa^* \ln \left(\frac{p'}{p_0} \right),$$

where

κ^* the modified swelling index.

The relationship between the elasticity modulus and Poisson's ratio is characterized by the following formula:

$$\frac{E_{ur}}{3(1-2\nu_{ur})} = \frac{p'}{\kappa^*},$$

where

E_{ur} the elastic unloading-reloading modulus,

ν_{ur} the Poisson's ratio for unloading-reloading.

κ^* is defined by the Mohr-Coulomb law and the pre-consolidation stress.

5. Examination

From the several data processed we have chosen the results from an examination at Tatabánya (firm clay, the unit weight is 21 kN/m^3). From the triaxial test the cohesion is $c = 68 \text{ kPa}$, and the friction angle is $\phi = 18^\circ$. In the *Fig. 4* you can see stress-strain formula in case of the soft-soil model in a semi-logarithmic scale. This semi-logarithmic scale makes the results linear. The input parameters of this model are obtained from compression tests. It is also suited for loading and unloading-reloading examinations. The usual ratio between λ^* and κ^* is three.

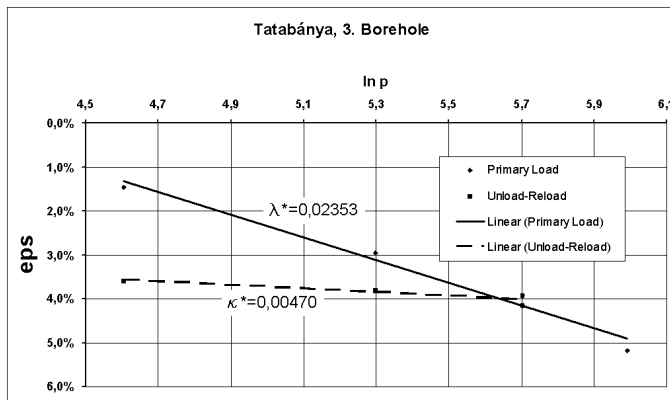


Fig. 4. Soft-Soil model stress-strain formula in case of compression test

The following figure shows the stress-strain model in case of the hardening soil model (*Fig. 5*). The Mohr-Coulomb yield condition is also applied here. Both stress and strain are depicted in a logarithmic scale. As we can see the Young's modulus is increasing in proportion with the power of stress. The value of the

Young's modulus comes from triaxial tests and the oedometric stiffness comes from compression tests. The sigma-epsilon dependency of the triaxial test, in this case, is hyperbolic. The unloading-reloading modulus (E_{ur}) varies as a function of σ_3' similarly to the E_{50} modulus.

Fig. 6 shows the stiffness-total stress dependency in case of triaxial tests. We can see that the greater the initial value of σ_3 the greater the Young's modulus is.

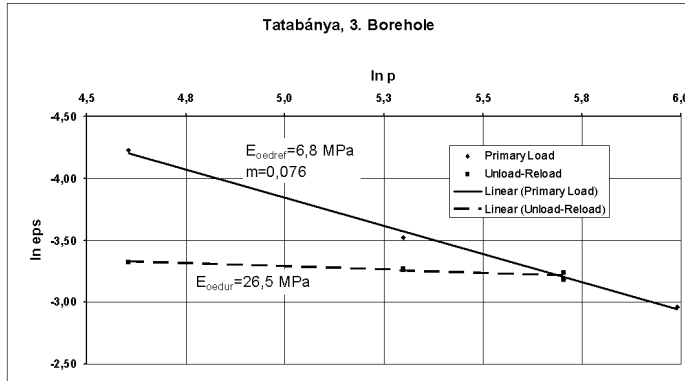


Fig. 5. Hardening-Soil model stress-strain formula in case of compression test

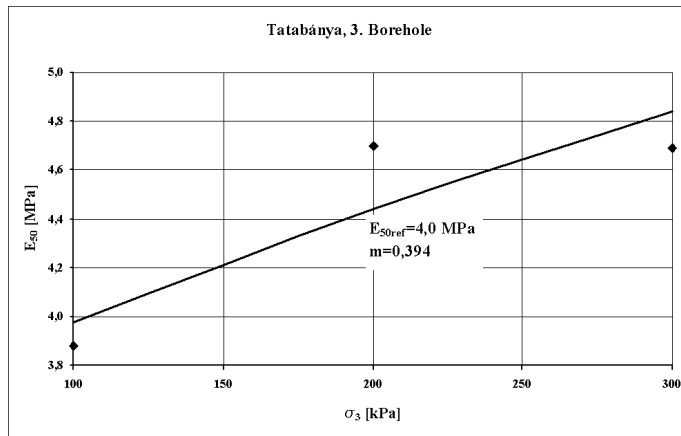


Fig. 6. Hardening-Soil model stiffness-total stress dependency in case of triaxial test

To test the results we used the PLAXIS 7.2 finite element code where we examined stability of cuttings and embankments. The finite element net is made up of 15-node (4th order) triangular elements (Fig. 7).

In the following figure you can see the finite element model of a cutting and the deformation in all three models (Fig. 8). Differences are present for both the

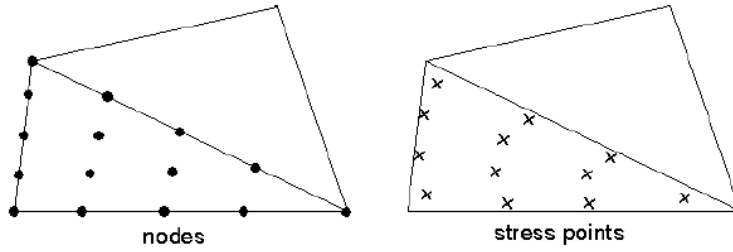


Fig. 7. Triangular element

shape and the volume of deformation. In case of the Mohr-Coulomb model the displacement is approximately parallel, in case of the hardening soil model it is leaning away from the wall while it is leaning towards the wall in case of the soft-soil model. The shape of the soil wall under examination is important because during construction it needs to be supported and we need to know the distribution of forces.

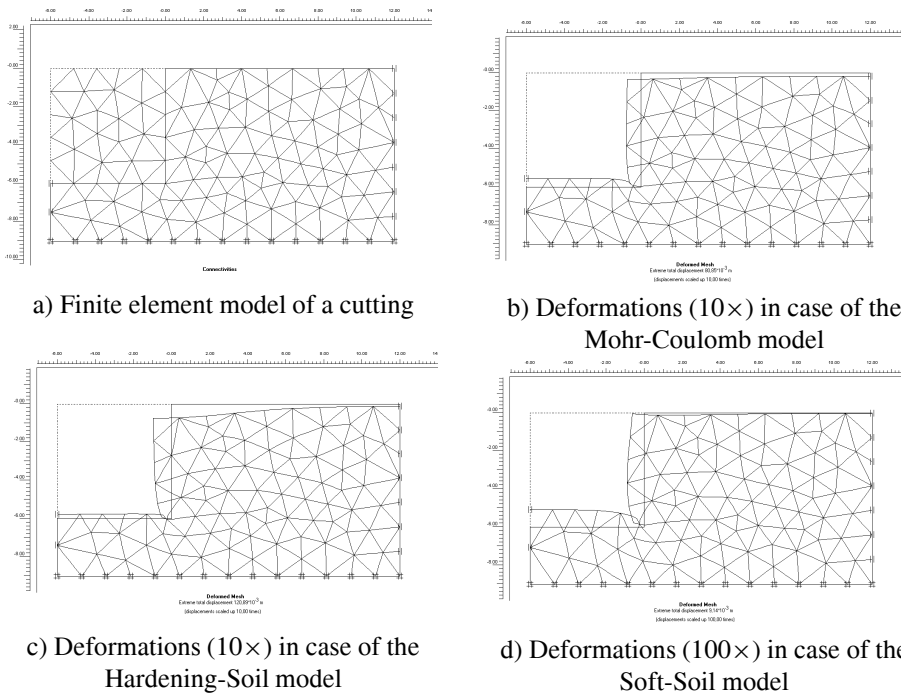


Fig. 8. The definition of the Young's modulus

The volume of deformations in the figure has been magnified for view ability.

In case of the soft-soil model deformations are much smaller than that of the other two models.

In case of cuttings we have compared the volume of displacements. The horizontal displacement is shown as a function of depth (*Fig. 9*). The displacements in case of the soft soil model are smaller by an order.

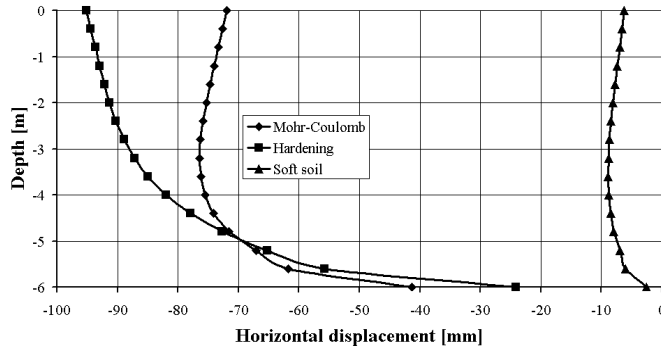


Fig. 9. Comparison of displacements in case of a cutting

Fig. 10 shows a model of an embankment. The embankment, the height of which is the same as the cutting examined above, is substituted by a uniform load, so that the parameters of the embankment do not influence the results. We have inserted an interface element into the singular point of the load. An interface element makes possible to have different displacements on its two sides, which avoids the formation of unbearable tension in the soil. Differences are present for both the shape and the volume of deformation. We have experienced the smallest deformations in case of the soft-soil model while the MC model showed some surface elevation.

Fig. 11 shows the settlement for embankments where the difference in deformations are also significant.

Safety factors have been defined for all three models in a way that we have decreased the shearing capacity until we experienced infinitely great deformations. The n_r is the reduction factor. The *Fig. 12* depicts the soil fracture in case of embankments and cuttings. Different colours show different volume of deformations. Although this figure shows the formation of a fracture for the MC model it is very similar to the other two models since all three models work according to the MC fracture condition.

$$\text{tg } \phi_r = \frac{\text{tg } \phi}{n_r}; \quad c_r = \frac{c}{n_r}; \quad n = \max(n_r)$$

Table 1 contains the safety parameters for different models in case of cuttings

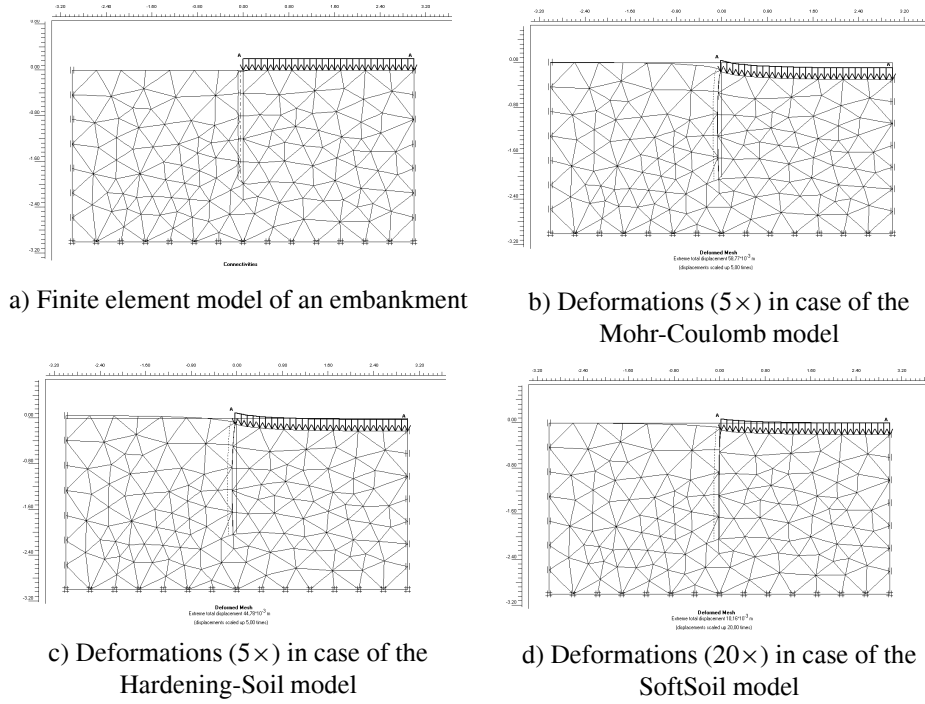


Fig. 10. Examination of an embankment

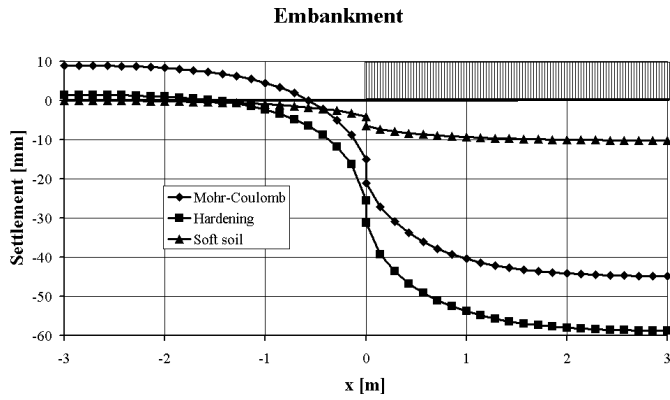


Fig. 11. Comparison of displacements in case of an embankment

and embankments. We can conclude that the safety parameters are approximately the same for each model but in case of embankments it is twice as in case of cuttings.

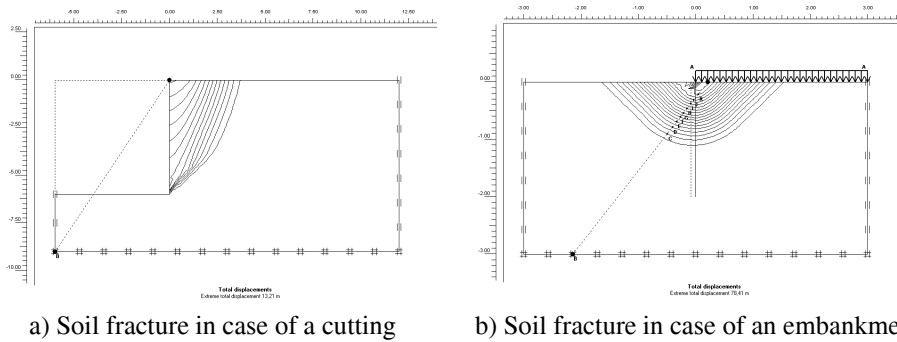


Fig. 12. Soil fracture modelling by Plaxis

Table 1. Safety factors

	Cutting	Embankment
Mohr-Coulomb	1.741	3.959
Hardening-Soil Model	1.719	3.884
Soft-Soil model	1.731	3.909

6. Summary

The difference in the safety parameter can be explained by the fact that cutting is an expansion while embankment is a compression for soil. Although the soil mechanics parameters are the same, expansion is a small deformation while compression is a significant deformation (Fig. 13). Thus in cases of the same load embankments have greater safety parameters than cuttings.

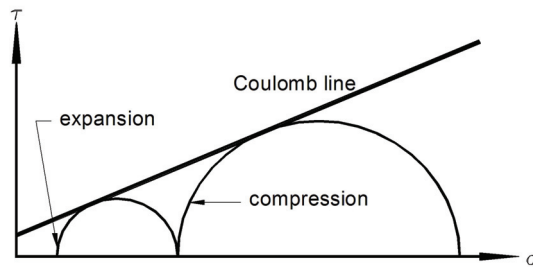


Fig. 13. Two alternatives of soil fracture

The difference shown in *Figs. 9* and *11* is more significant. We have applied three different soil models that are frequently used in recent investigations all around the world. Their parameters have been defined by the same laboratory examinations but still the resulting soil deformations significantly differ.

One possible cause of this difference is that we made use of the results of triaxial tests when applying the Mohr-Coulomb and the Hardening Soil models while in case of the Soft Soil Model we only used the results of the compression test. Based on these findings we may conclude that the similar results of the first two tests are more reliable. Nevertheless, experience shows that real deformations are significantly less than the calculated results, which may support the third model.

To resolve this contradiction we firstly need to do further tests that provide statistically sufficient volume of data. Secondly, we need to compare the test results with real-life deformation data.

References

- [1] BRINKGREVE, R. B. – VERMEER, J., *PLAXIS-Finite Element Code for Soil and Rock Analyses, Version 7*. A. A. Balkema, Rotterdam, Brookfield, 1998.
- [2] FREISEDER, M. G. – SCHWEIGER, H. F., Numerical Analysis of Deep Excavations, *Proceedings of Application of Numerical Methods to Geotechnical Problems*, Udine, 1998. pp. 283–292.
- [3] BIRÓ, V. – CZAP, Z., Sheet Pile Wall Measurement with up-to-date Numerical Methods, *GÉP*, **50** (5) (1999), pp. 24–26.
- [4] CZAP, Z., *Modern Constitutive Models in Geotechnics, microCAD'99*, Miskolc, 1999.
- [5] CZAP, Z., Geotechnikai szoftverek összehasonlítása, Geotechnika 2002 Conference, Ráckeve, 2002.